Next Nanotechnology 7 (2025) 100136

Contents lists available at ScienceDirect

Next Nanotechnology

journal homepage: www.sciencedirect.com/journal/next-nanotechnology

Research article

Novel green synthesis of silver nanoparticles from empty fruit bunch waste: Biomedical applications and mechanistic insights

Bashirat Olamide Yusuf-Salihu [a,*], Shakirat Afodun Abdulmumini [a], Toheeb Taiye Bajepade [a], Halimah Adekunbi Durosinmi [a], Muinat Olanike Kazeem [b], Victoria Atinuke Ajayi [c], Agbaje Lateef [d]

[a] Department of Microbiology, Kwara State University, Malete, Kwara State, Nigeria
[b] Department of Microbiology, Faculty of Life Sciences, University of Ilorin, Kwara State, Nigeria
[c] Department of Science Laboratory Technology, Ladoke Akintola University of Technology, Ogbomoso PMB 4000, Nigeria
[d] Laboratory of Industrial Microbiology and Nanobiotechnology, Ladoke Akintola University of Technology, PMB 4000, Ogbomoso, Nigeria

ARTICLE INFO

Keywords:
Empty Fruit Bunch
Silver nanoparticles
Green synthesis
Anticoagulant
Antimicrobial activity
Antioxidant activity

ABSTRACT

Agricultural waste, such as empty fruit bunches (EFB) from palm oil production, poses environmental and health risks if not effectively managed. This study addresses this issue by innovatively transforming EFB biomass into high-value silver nanoparticles (AgNPs) via a green synthesis approach, marking the first successful biosynthesis of AgNPs from EFB. UV-Vis, FTIR, TEM, SAED, and EDX studies were used to characterize biosynthesized EFB-AgNPs. Biosynthesized EFB-AgNPs were tested for antibacterial, antioxidant, antidiabetic, anticoagulant, and thrombolytic activities. EFB-AgNPs showed a surface plasmon resonance peak at 477 nm, hydroxyl and amine group stabilization, and a silver content of 75.56 %. TEM and SAED analyses confirmed nanoscale particle diameters ranging from 12.78 nm to 19.10 nm, with a characteristic face-centered cubic (FCC) crystalline structure. EFB-AgNPs inhibited *Escherichia coli*, *Klebsiella oxytoca*, *Staphylococcus aureus*, *Proteus mirabilis*, and *Pseudomonas aeruginosa* dose-dependently from 40 % to 80 %, and 100 % of *Aspergillus niger*, *A. fumigatus*, and *A. flavus*. Reactive oxygen species (ROS) may cause cell membrane rupture and oxidative stress. Antioxidant testing demonstrated concentration-dependent activity across multiple assays: DPPH scavenging reached 81.49 % at 160 μg/ml, ferric-reducing activity was 90.05 % at 150 μg/ml, H_2O_2 scavenging achieved 91.00 % at 80 μg/ml, and NO scavenging reached 83.43 % at 150 μg/ml. Furthermore, EFB-AgNPs prevented blood coagulation and dissolved blood clots. In addition, EFB-AgNPs inhibited α-amylase with 74.64 % at 100 μg/ml. This unique approach of transforming EFB trash into high-value AgNPs could help sustain waste management and the circular bioeconomy by enabling medicinal applications.

1. Introduction

Nanotechnology has significantly impacted various industries, especially medicine, by producing nanoparticles with unique properties and diverse biological activities. Silver nanoparticles (AgNPs) have emerged as appealing nanomaterials owing to their potent antibacterial properties, effective against a wide range of pathogens, including bacteria, fungi, and viruses. The unique physicochemical properties of AgNPs, such as their high surface area-to-volume ratio and ability to release silver ions, augment their efficacy as antibacterial agents [46,56,62,79,93]. Recent research have underscored the potential of AgNPs in several biomedical applications, including wound healing, dental materials, and drug delivery systems, emphasizing their adaptability and importance in modern medicine [42,92,94].

The green synthesis of metallic nanoparticles has emerged as a significant area of research, particularly in the context of sustainable development and environmental conservation. This approach utilizes biological materials, such as plant extracts, to produce nanoparticles in a manner that is eco-friendly, cost-effective, and efficient. Recent studies have highlighted the advantages of using plant extracts for the synthesis of various metallic nanoparticles, exhibiting unique properties suitable for diverse applications in medicine, environmental remediation, and catalysis [61,71,82]. The process of green synthesis not only minimizes the environmental impact associated with traditional chemical methods

* Corresponding author.
E-mail address: bashirat.yusuf@kwasu.edu.ng (B.O. Yusuf-Salihu).

https://doi.org/10.1016/j.nxnano.2025.100136
Received 23 September 2024; Received in revised form 16 December 2024; Accepted 13 January 2025
2949-8295/© 2025 The Author(s). Published by Elsevier Ltd. This is an open access article under the CC BY-NC-ND license (http://creativecommons.org/licenses/by-nc-nd/4.0/).

but also enhances the stability and biocompatibility of the nanoparticles produced. For instance, the use of plant extracts as reducing and stabilizing agents has been shown to facilitate the formation of nanoparticles with controlled size and morphology, which is crucial for their effectiveness in various applications [9,76,64]. Recent studies have highlighted the advantages of this method, particularly in the synthesis of silver nanoparticles (AgNPs), which have demonstrated significant antimicrobial properties. The green synthesis of AgNPs using extracts from plants such as *Cannabis sativa*, Kemloko fruit, and *Moringa oleifera*, among others have been reported to yield nanoparticles with potent antibacterial activities, making them valuable in medical and environmental applications [18,59,8].

The plant extracts are abundant in phytochemicals that promote the reduction of silver ions to nanoparticles, while also providing other biological activities, including antioxidant and anti-inflammatory effects [48,68,91]. The dual functionality increases the therapeutic potential of AgNPs, rendering them appropriate for various applications in biomedicine. Moreover, the environmental consequences of producing AgNPs from agricultural waste, such as EFB, must not be disregarded. Using waste materials enhances sustainability and mitigates the environmental impact of conventional nanoparticle manufacturing techniques. This methodology is consistent with the tenets of green chemistry, advocating for environmentally sustainable methods in nanotechnology [103,35,83]. Researchers can employ agricultural by-products to create economical and eco-friendly techniques for synthesizing AgNPs, thereby mitigating health and environmental issues.

The characterization of AgNPs is crucial for understanding their size, shape, and surface properties, which directly influence their biological activities. Methods including UV-Vis spectroscopy, transmission electron microscopy (TEM), and dynamic light scattering (DLS) are frequently utilized to examine the produced nanoparticles [24,6,86,98,99]. Recent studies indicate that the dimensions and morphology of AgNPs substantially influence their antibacterial efficacy, with smaller nanoparticles demonstrating superior activity owing to their augmented surface area and capacity to infiltrate microbial cell membranes [70,72]. Furthermore, the stability of AgNPs in biological contexts is essential for their practical uses, requiring the investigation of diverse stabilizing agents and formulations [11,54]. Besides their antimicrobial capabilities, AgNPs exhibit considerable antioxidant activity, crucial for alleviating disorders associated with oxidative stress. The antioxidant potential of AgNPs is frequently ascribed to the phytochemical constituents of the plant extracts employed in their manufacture, which can neutralize free radicals and safeguard cellular components from oxidative harm [84,95]. This feature is especially significant in the realm of chronic disorders, wherein oxidative stress is important in disease advancement. Research indicates that AgNPs derived from diverse plant extracts demonstrate preventive properties against oxidative damage in cellular models [68,84].

The antidiabetic efficacy of AgNPs has been investigated, with multiple studies demonstrating its capacity to modulate blood glucose levels and enhance insulin sensitivity. The AgNPs derived from the foliage of medicinal plants have demonstrated hypoglycemic effects in diabetic animal models, indicating their potential as supplementary treatments in diabetes care [69,79]. The diverse therapeutic potential of AgNPs renders them significant candidates for tackling numerous health issues, including metabolic disorders. Additionally, the anticoagulant characteristics of AgNPs have attracted interest recently, especially concerning cardiovascular health. The capacity of AgNPs to influence coagulation pathways and improve fibrinolytic activity offers an innovative strategy for preventing thrombus formation and managing cardiovascular diseases [31,41]. Studies have demonstrated that AgNPs can significantly impede platelet aggregation and enhance blood circulation, underscoring their promise as therapeutic agents in vascular medicine [29,70].

Empty fruit bunches (EFB), a derivative of palm oil manufacturing, have traditionally been underexploited, as prevalent methods like composting or utilizing it as low-grade fuel do not fully harness their potential [27]. Due to the rich components like lignin, cellulose, and hemicellulose found in EFB, researchers have repurposed it for creative applications, including biochemical synthesis and biofuel production, by the ideals of a circular bioeconomy and sustainable development [60,78,87]. The ample availability of EFB as a raw material for biochemical synthesis or biofuel production underscores its significance in the transition to sustainable practices [23]. Moreover, the transformation of EFB fibers into cellulose and carboxymethylcellulose (CMC), along with the separation of lignin, underscores the adaptability of lignocellulosic agro-industrial leftovers for generating higher-value products [34,36]. EFB can generate organic acids and other value-added products via recovery and purification processes, hence underscoring the versatility of this lignocellulosic material [102]. Additionally, EFB has been exploited in co-firing power plants using torrefaction procedures which emphasizes its potential contribution to renewable energy generation [88]. A thorough examination of biofuels derived from EFB highlights the present condition, potential, obstacles, and future directions for utilizing this biomass in sustainable biofuel production [37]. The production of bioethanol from EFB and the characterization of low-ash EFB pellets as solid biofuels illustrate the varied possibilities of this agricultural waste in the renewable energy sector [65]. The catalytic co-pyrolysis of EFB and coal into liquid oil underscores the potential for efficient and environmentally friendly alternative energy sources [40].

Despite the abundance of bioactive chemicals found in EFB and the applications above, its utilization in nanotechnology and biological domains remains unexplored. Employing EFB not only offers a beneficial application for this waste material but also adheres to the tenets of green chemistry by diminishing dependence on hazardous substances. This study builds upon the green synthesis of AgNPs by utilizing EFB extract for the first time. The synthesized nanoparticles were described using various methods, and their biological activities were evaluated. The antimicrobial efficacy of AgNPs against several bacterial and fungal isolates was assessed via turbidimetric and poisoned plate methodologies respectively. Furthermore, the nanoparticles' antioxidant, antidiabetic, anticoagulant and thrombolytic activities were assessed to evaluate their potential as multifunctional agents in biomedical applications. The study also explores the mechanisms behind AgNPs' biological activities, aiming to deepen understanding of their effects and safety in therapeutic applications.

2. Materials and methods

2.1. Materials

Chemicals and other reagents used in this study were procured from K-Prime Medics Integrated Limited, with all reagents being of analytical grade and at least 99 % purity.

2.2. Preparation of EFB Extract

The EFB was acquired from a private oil processing firm situated in Ilorin, Kwara State, Nigeria (8.47239° N, 4.58107° E). The EFB samples were air-dried at room temperature and then milled. The milled samples were then extracted with water at 60 °C for one hour using a 1 % (wt/vol) solution. After extraction, the solution was filtered using Whatman filter paper No. 1 and centrifuged at 4000 rpm for 20 minutes. The resulting extracts were employed immediately without further purification [101].

2.3. Silver nanoparticle phytosynthesis and characterization

Precisely 1 ml of the filtered EFB extract was introduced into a reaction tube containing 40 ml of a 1 mM $AgNO_3$ solution. The reaction was conducted at ambient temperature (30 ± 2 ℃), with color changes visually monitored over 24 hours [100]. Subsequently, the absorption

spectrum was analyzed by scanning within the 200–800 nm range using a UV-Vis spectrophotometer. The biosynthesize AgNPs were further examined utilizing Fourier transform infrared spectroscopy (Nicolet iS10 FTIR Spectrometer), transmission electron microscopy (JEM-ARM200F-G TEM JOEL-JSM 7600 FJ), energy-dispersive X-ray spectroscopy, and scanning electron microscopy (JOEL-JSM 7600 FJ).

2.4. Antimicrobial efficacy of the biosynthesized EFB-AgNPs

The antibacterial efficacy of the biosynthesized EFB-AgNPs was assessed by a broth dilution assay [49], employing multi-drug resistant gram-positive and gram-negative bacterial isolates (*Escherichia coli, Klebsiella oxytoca, Staphylococcus aureus, Pseudomonas aeruginosa,* and *Proteus mirabilis*) obtained from the University of Ilorin Teaching Hospital, Oke-Oyi, Nigeria. One milliliter of each 24-hour broth culture, calibrated to a 0.5 McFarland standard (1 ×10^6 cfu/ml), was inoculated into 8 milliliters of peptone broth. Thereafter, 1 ml of EFB-AgNPs at concentrations of 20, 40, 60, 80, and 100 μg/ml was included in the mixture. The control lacked nanoparticles. The cultures were maintained at 37 °C for 24 hours. Subsequent optical density measurements were conducted at 600 nm, and the percentage of growth inhibition was calculated accordingly using the formula below:

$$\%\ \text{Growth inhibition} = \frac{OD\ Control - OD\ Test}{OD\ Control} \times 100 \quad (1)$$

where OD is optical density.

The antifungal efficacy of the EFB-AgNPs was assessed by a mycelial growth inhibition test [49]. The EFB-AgNPs were included in potato dextrose agar (PDA) at concentrations of 100 and 150 μg/ml, followed by inoculation with 6 mm agar plugs from 48-hour-old cultures of *Aspergillus flavus*, *Aspergillus fumigatus*, and *Aspergillus niger*. The control plates were devoid of nanoparticles. All plates were incubated at 28 ± 2 °C for a duration of 72 hours. The diameters (D) of fungal growth were measured in millimeters, and the percentage of growth inhibition was calculated correspondingly as follows:

$$\%\ \text{Growth inhibition} = \frac{OD\ Control - OD\ Test}{OD\ Control} \times 100 \quad (2)$$

where OD is optical density.

2.5. Potential mechanism of action of the biosynthesized EFB-AgNPs

The procedure use was derived from the methodology of Aguda and Lateef [6]. Attempts were made to clarify the possible mechanisms of action of the nanoparticles against the bacterial isolates employed. A sterile peptone solution (6 ml) was prepared, to which 1 ml of a 24-hour-old culture of the test isolates was included, along with 1 ml of nanoparticles at concentrations of 100 μg/ml and 150 μg/ml (individually). The resultant mixture was subsequently incubated for 24 hours at 37°C. A control broth culture was established without including nanoparticles. Subsequent to incubation, the cultures are subjected to centrifugation at 4000 rpm for 15 min, and the optical density of the supernatant is evaluated at 260 nm and 280 nm to determine the presence of DNA and proteins, respectively.

2.6. Anticoagulant and thrombolytic activity of the biosynthesized EFB-AgNPs

The anticoagulant assay was performed according to the methodology outlined by Oladipo et al. [67]. In this assay, 1 ml of EFB-AgNPs at a concentration of 100 μg/ml was combined uniformly with blood from a healthy donor in a sterile Eppendorf tube. Blood was collected in an EDTA bottle for the positive control, whereas the negative controls consisted solely of blood samples collected in a sterile Eppendorf tube. The samples were allowed to rest for up to one hour, during which visual assessments were conducted to detect any blood coagulation. To confirm the results, each Eppendorf tube was inverted to assess the presence of anticoagulation. The contents of the tube were then placed on a slide and examined under an optical microscope to detect the red blood cells, following the approach outlined by Azeez et al. [16].

Thrombolytic activity was evaluated using a method outlined by Oladipo et al. [67] for both qualitative and quantitative assessments. In this procedure, 0.1 ml of blood was transferred into a pre-weighed, sterile Eppendorf tube and incubated at 37 °C for 30 minutes to promote clot formation. Subsequent to clot formation, the tube was re-weighed, and the mass of the blood clot (denoted as X) was determined by subtracting the initial mass of the tube. The coagulated blood was then treated with 1000 μl of EFB-AgNPs. The tubes were incubated at 37 °C for 90 minutes and then evaluated for signs of thrombolysis. Each tube was inverted to separate the lysed clot from the non-lysed clot. The final weight of the tube, including the residual blood clot, was recorded, and the initial weight of the tube was subtracted to determine the weight of the non-lysed blood clot (marked as Y). The thrombolytic activity was measured as follows:

$$\textit{Thrombolytic activity} = \frac{X - Y}{X} \times 100 \quad (3)$$

2.7. In vitro antioxidant activities of the biosynthesized EFB-AgNPs

To evaluate the antioxidant activity of the biosynthesized EFB-AgNPs, the DPPH (2,2-diphenyl-1-picrylhydrazyl) test, H_2O_2 (hydrogen peroxide scavenging) assay, FRAP (ferric-reducing antioxidant power) assay, and NO (nitric oxide) assay were utilized, following the established methodology [101].

Different concentrations (100–160 μg/ml) of EFB-AgNPs were assessed in the DPPH assay. Solutions of EFB-AgNPs were prepared at various concentrations (100–160 μg/ml) and mixed with 4 ml of a 1 mM DPPH solution. The mixture was incubated in the dark for 30 minutes to stabilize free radical interactions. Ascorbic acid served as the reference standard. Absorbance was measured at 517 nm using a UV-Vis spectrophotometer (Spectro UV-2505). The % DPPH scavenging activity was calculated using the formula:

$$\%\textit{DPPH scavenging effect} = \frac{AB - AS}{AB} x100 \quad (4)$$

Where: AB= Blank's absorbance and AS= Sample's absorbance.

To carry out H_2O_2 assay, A 40 mM solution of H_2O_2 was prepared using phosphate buffer (pH 7.4). EFB-AgNPs were tested at various concentrations (10–80 μg/ml). Specifically, 0.6 ml of the H_2O_2 solution was mixed with 4 ml of distilled water and varying amounts of the nanoparticles. The mixture was incubated for 20 minutes, after which absorbance was measured at 610 nm using a UV-Vis spectrophotometer (Spectro UV-2505). Ascorbic acid was used as the reference standard. The scavenging activity was calculated using the following formula:

$$\%\ H_2O_2\ \text{scavenging effect} = \frac{AC - AS}{AC} x100 \quad (5)$$

Where AC represents the absorbance of the negative control, and AS denotes the absorbance of the sample.

For ferric reducing antioxidant power of the biosynthesized EFB-AgNPs. EFB-AgNPs were evaluated at different concentrations (10, 20, 40, 60, 80, 100, and 150 μg/ml), with ascorbic acid serving as the standard reference. For each sample, 2.5 ml of 200 mM phosphate buffer (pH 6.6) and 2.5 ml of 1 % potassium ferricyanide were added. The mixtures were incubated at 50°C for 20 minutes and rapidly cooled. Next, 2.5 ml of 10 % trichloroacetic acid (TCA) was added to terminate the reaction, followed by centrifugation at 3000 rpm for 10 minutes. The supernatant (2.5 ml) was combined with 2.5 ml of deionized water and 1 ml of 0.1 % ferric chloride solution. Absorbance was measured at 700 nm using a UV-Vis spectrophotometer (Spectro UV-2505). A blank

devoid of nanoparticles was used as a control. The reducing activity was calculated using the formula:

$$\%\ \text{reducing activity} = \frac{A_{sample} - A_{blank}}{A_{blank}} x100 \quad (6)$$

where A is Absorbance

Different concentrations of EFB-AgNPs (10–150 μg/ml) were prepared, with ascorbic acid serving as the standard reference for the nitric oxide scavenging assay. A 5 mM sodium nitroprusside solution in phosphate-buffered saline (pH 7.4) was used to generate nitric oxide (NO) radicals. One milliliter of sodium nitroprusside solution was mixed with varying concentrations of EFB-AgNPs and incubated at 25°C for 30 minutes. Following incubation, 2 ml of Griess reagent (1 % sulfanilamide, 2 % phosphoric acid, and 0.1 % N-1-naphthyl ethylenediamine dihydrochloride) was added to the reaction mixture to detect nitrite formed from NO. Absorbance was measured at 546 nm using a UV-Vis spectrophotometer (Spectro UV-2505). The nitric oxide scavenging activity was calculated using the following formula:

$$\%\ \text{scavenging effect} = \frac{AC - AS}{AC} x100 \quad (7)$$

Where: AC= absorbance of control and AS= absorbance of sample

2.8. In vitro anti-diabetic assay

2.8.1. α-Amylase inhibitory activity

The *in vitro* antidiabetic efficacy of biosynthesized EFB-AgNPs (concentrations 20–100 μg/ml) was assessed using a conventional α-amylase technique [101]. Various concentrations of EFB-AgNPs (20, 40, 60, 80, and 100 μg/ml) were tested, with acarbose serving as the standard reference. To conduct the assay, 500 μl of each EFB-AgNPs concentration was mixed with 500 μl of 0.2 mM phosphate buffer (pH 6.9) containing α-amylase solution (0.5 mg/ml). The reaction mixture was incubated at room temperature for 10 minutes, followed by the addition of 500 μl of a 1 % starch solution in 0.02 M sodium phosphate buffer (pH 6.9). The reaction was allowed to proceed for another 10 minutes and was terminated by the addition of 1 ml of 3,5-dinitrosalicylic acid (DNS) reagent. The reaction mixtures were heated in a boiling water bath for 5 minutes, cooled to room temperature, and diluted with 10 ml of distilled water. Absorbance was measured at 540 nm using a UV-Vis spectrophotometer (Spectro UV-2505). A control sample was prepared without EFB-AgNPs. The percentage inhibition of α-amylase activity was calculated using the formula:

$$\%\text{inhibition} = \frac{AC - AS}{AC} x100 \quad (8)$$

Where: AC represents the absorbance of the control, and AS denotes the absorbance of the sample.

2.9. Statistical analysis

All experimental results were statistically analyzed using SPSS Version 27.0 statistical software. Data were expressed as mean ± standard error (SE) and were derived from three independent experiments conducted triplicate, depending on the assay. Significant differences among experimental groups were determined using one-way analysis of variance (ANOVA), followed by Duncan's post-hoc test to compare the means and highlight significant variations among samples. A p-value < 0.05 was considered statistically significant.

3. Results and discussion

3.1. Biosynthesis of AgNPs

In the production of AgNPs utilizing EFB extract, a notable color change occurred in the $AgNO_3$ solution, shifting from colorless immediately upon mixing to a deep dark brown as the reaction reached equilibrium (Fig. 1a). This change, took place within one hour and stabilizing over 24 hours, is indicative of effective nanoparticle production. Color alterations have been documented in the phytosynthesis of nanoparticles [24,6,100]. Numerous researchers have recorded these color differences, indicating the variability in nanoparticle synthesis circumstances and the properties of the final product. The dark brown hue noted in this investigation signifies the establishment of a stable colloidal suspension of AgNPs. The hue and intensity can yield information regarding the dimensions, distribution, and concentration of the nanoparticles, that are influenced by the distinctive phytochemicals in the EFB extract. The bioactive chemicals in the extract function as bioreductants, enabling the reduction of silver ions to nanoparticles and influencing the unique features of the generated AgNPs. The brown hue exhibited by the EFB-AgNPs is a notable feature among the diverse colors of AgNPs documented in the literature, which include light yellow, brown, and dark brown tones [26,44].

3.2. Characterization of the biosynthesized EFB-AgNPs

The λmax of the biosynthesized EFB-AgNPs was observed at 477 nm with an absorbance of 0.7621, as illustrated in Fig. 1b, indicating the existence of nanoparticles and associated with the phenomenon of surface plasmon resonance (SPR), characterized by the collective oscillation of free electrons at the surface of metallic nanoparticles when excited by incident light. AgNPs exhibit SPR predominantly within the observable spectrum, often ranging from 400 nm to 500 nm, influenced by variables such as particle size, morphology, and the surrounding medium [20]. Literature indicates that authors have documented λmax values between 400 and 500 nm for biosynthesized AgNPs [74,85]. The absorption peak at 477 nm signifies the production of AgNPs. This peak indicates the reduction of silver ions (Ag^{+}) to metallic silver (Ag^{0}), implying that the nanoparticles are uniformly scattered in the solution. The absorbance values near the peak at 477 nm signify stable nanoparticle formation. At 475 nm: 0.7619, 476 nm: 0.7620, 477 nm: 0.7621, 478 nm: 0.7621, and at 479 nm: 0.7620, indicating a relatively consistent size distribution of the nanoparticles. Additionally, a broad absorption band extending from 350 to 650 nm was observed, which is a characteristic feature of nanoparticles with diverse size distributions and morphological variations. Such broadening in the SPR band has been previously reported in green-synthesized AgNPs, where the complexity of reducing and stabilizing agents in plant extracts influences the size, shape, and aggregation state of nanoparticles [30]. In this study, phytochemicals in the EFB extract likely acted as reducing and capping agents, influencing nanoparticle nucleation and growth. This resulted in irregular shapes and a size distribution as confirmed by TEM analysis.

The FTIR spectrum of biosynthesized EFB-AgNPs indicates essential functional groups implicated in their synthesis and stability (Fig. 2). The notable peak at 3383.40 cm is ascribed to O-H stretching vibrations of hydroxyl groups, in accordance with previous studies [43,45], indicating their function in reducing silver ions. A peak at 1638.19 signifies N-H bending vibrations of amine groups, corroborating previous findings by Lee et al. [50], demonstrating the function of proteins in the stability of nanoparticles. The peak at 410.35 corresponds to metal-oxygen (Ag-O) stretching vibrations. which are indicative of AgNPs. These vibrations indicate that the synthesis process successfully produced AgNPs, as these vibrations are generally linked to the bonding interactions between silver and oxygen atoms derived from the plant extract. The establishment of Ag-O bonds in AgNPs signifies efficient capping by constituents of plant extracts, which inhibits agglomeration and improves nanoparticle stability. The capping is essential for preserving the distinctive characteristics of AgNPs, as emphasized by Obiazikwor and Shittu [66] and Liaqat et al. [53], who observed that phytochemicals are instrumental in the reduction of silver ions and the

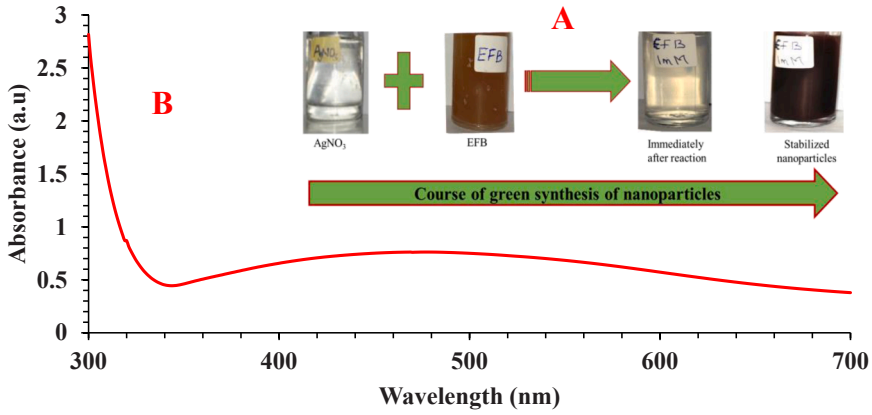


Fig. 1. The course of biosynthesis of EFB-AgNPs (A); SPR of the UV-Vis absorption of the biosynthesized EFB-AgNPs (B).

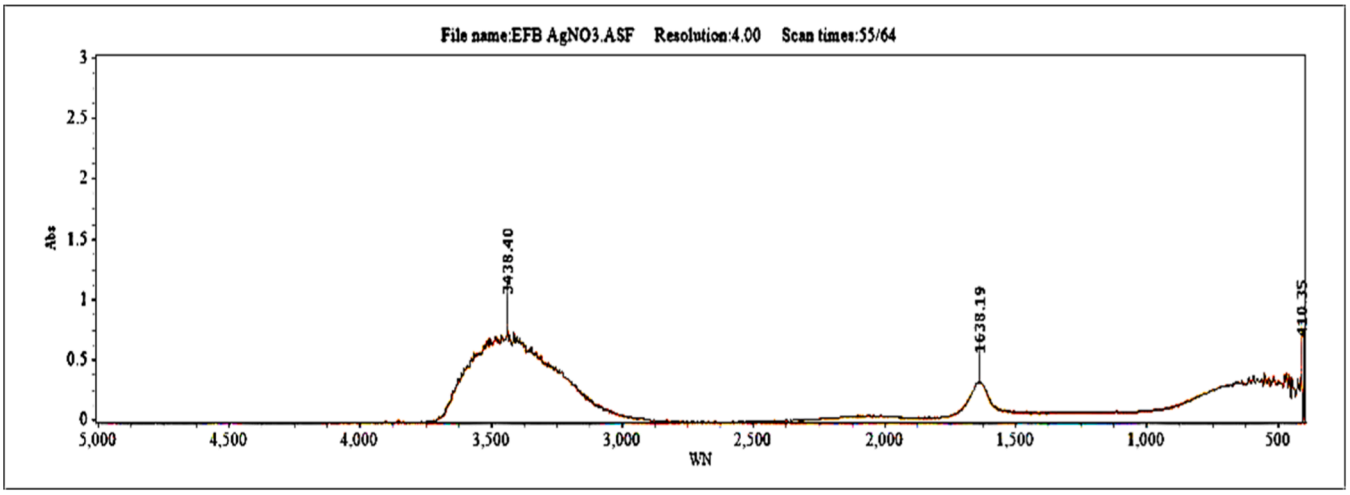


Fig. 2. FTIR spectra of biosynthesized EFB-AgNPs.

stabilization of nanoparticles.

The Energy Dispersive X-ray (EDX) analysis of EFB-AgNPs reveals a predominant silver (Ag) composition, constituting 75.56 % by weight and 60.20 % by atomic percentage, hence confirming successful nanoparticle production (Fig. 3a). Oxygen (O) is also important, probably because capping agents from the EFB extract possess oxygen-rich functional groups. Smaller amounts of carbon (C) and nitrogen (N) suggest the existence of organic molecules derived from the extract, aiding in nanoparticle reduction and stabilization. Sodium (Na) is present in trace amounts, potentially aiding in nanoparticle stability, whereas a modest silicon (Si) signal is ascribed to the substrate or contamination.

The Selected Area Electron Diffraction (SAED) pattern of biosynthesized silver nanoparticles (AgNPs) derived from empty fruit bunch (EFB) extract offers essential insights into their crystallinity and phase structure. The SAED pattern displays distinct bright spots organized in concentric rings, characteristic of polycrystalline materials (Fig. 3b). This configuration signifies multiple crystallographic planes, affirming that the EFB-AgNPs possess a crystalline structure typical of face-centered cubic (FCC) silver. The presence of these rings corresponds to specific crystallographic planes, which can be indexed to the (111), (200), (220), and (311) planes of FCC silver, as validated by various studies [14,89,97].

The TEM analysis of the biosynthesized silver nanoparticles (AgNPs) from empty fruit bunch (EFB) extract shows that the particles are mostly spherical, with sizes ranging from about 12.78 nm to 19.10 nm (Fig. 3c). Well-synthesized silver nanoparticles have a narrow size distribution and spherical shape. The fact that the EFB-AgNPs are dispersed well, as shown by the lack of agglomeration, suggests that the nanoparticles are stable. This is likely due to the phytochemicals present in the EFB extract, which can act as both reducing and stabilizing agents during the synthesis process. The presence of these biomolecules not only stabilizes the nanoparticles but may also make them more biocompatible and effective for a wide range of biomedical uses, such as drug delivery and antimicrobial therapies [3].

3.3. Antimicrobial efficacy of the biosynthesized EFB-AgNPs

3.3.1. Antibacterial activity

In this study, EFB-AgNPs exhibit significant broad-spectrum antibacterial activity against various bacterial strains, including *Escherichia coli*, *Klebsiella oxytoca*, *Staphylococcus aureus*, *Pseudomonas aeruginosa*, and *Proteus mirabilis* (Fig. 4). The observed inhibition rates varied between 40 % and 80 % across the tested bacterial strains, demonstrating a distinct dose-dependent effect when concentrations increased from 20 μg/ml to 100 μg/ml. Notably, *S. aureus* was the most sensitive, with up to 80 % inhibition at the highest concentration tested. This matches the results of [17], who found that *S. aureus* was similarly inhibited (61.29 %) at 50 μg/ml. Furthermore, [17] demonstrated the sensitivity of *S. marcescens* and *P. aeruginosa* to AgNPs, with inhibition rates of 59.34 % and 54.42 % at 50 μg/ml, respectively, which is consistent with our findings of 49 %-74 % inhibition for *P. aeruginosa*. The antibacterial efficacy observed may be attributed to mechanisms such as cell membrane disruption and oxidative stress induction by silver nanoparticles, as supported by additional mechanistic studies conducted here, which

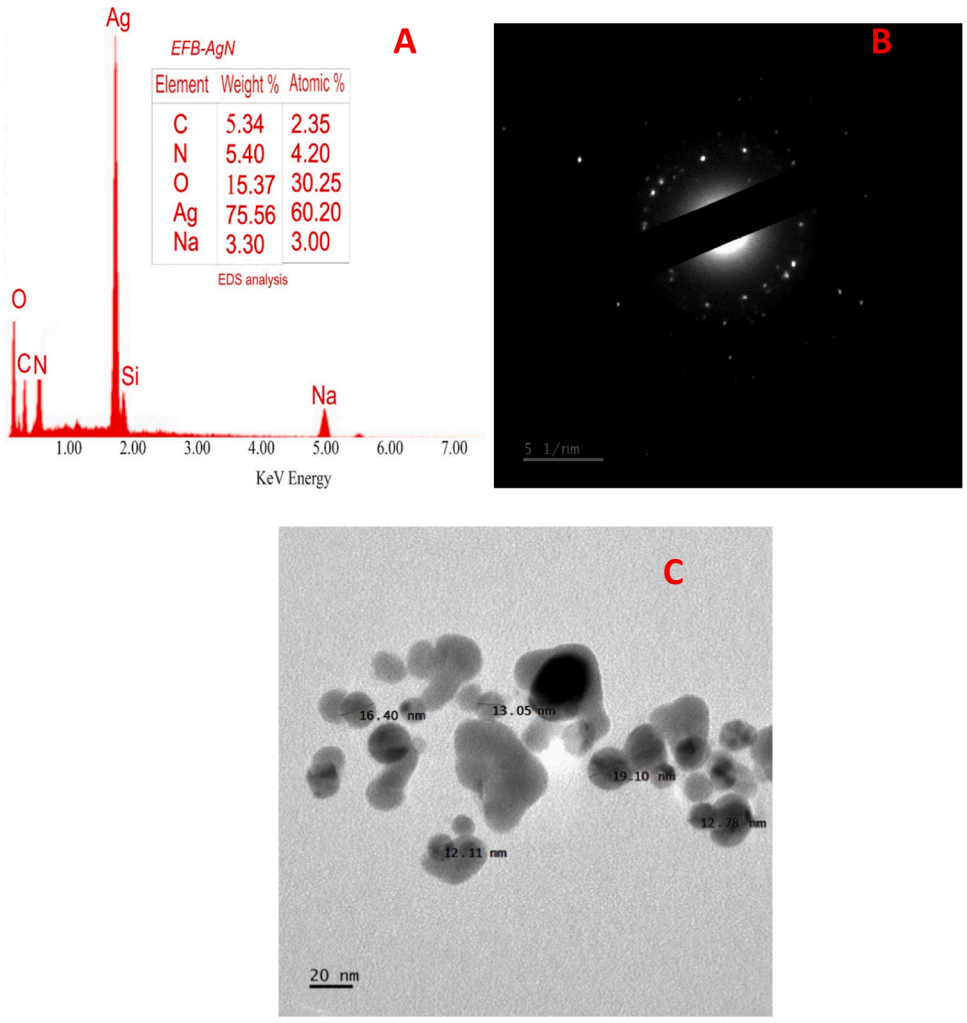


Fig. 3. EDX signals of biosynthesized EFB-AgNPs (A); SAED patterns of biosynthesized EFB-AgNPs (B); TEM micrographs of the biosynthesized EFB-AgNPs (C).

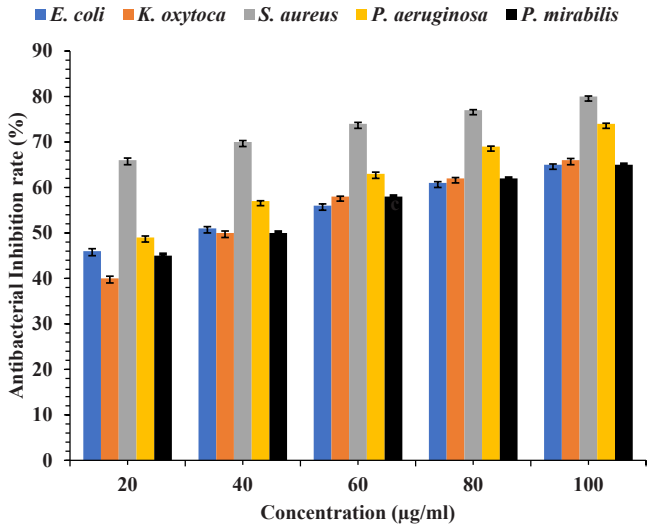


Fig. 4. Antibacterial activity of EFB-AgNPs against various bacterial strains at different concentrations. Data are presented as mean ± SE from three independent experiments performed in triplicate. Statistical significance was determined by ANOVA with Duncan's test for mean comparison ($p < 0.05$). Error bars indicate the standard error of the mean.

will be discussed in a later section. Statistical analysis confirmed that the observed differences across bacterial strains and concentrations were significant ($p < 0.05$), reinforcing the potential of EFB-AgNPs as antimicrobial agents. These results align with previous research emphasizing the antibacterial potency of AgNPs against both Gram-positive and Gram-negative bacteria [33,38,6,96,100].

3.3.2. *Antifungal activity*

The antifungal efficacy of EFB-AgNPs exhibited total suppression of the fungal strains *A. niger, A. fumigatus*, and *A. flavus* at concentrations of 100 and 150 mg/ml (Fig. 5). This discovery underscores the potential of EFB-AgNPs as a viable antifungal drug, especially given the rising resistance of fungi to traditional antifungal therapies. The findings correspond with prior research that has recorded the antifungal efficacy of AgNPs against many fungal infections, including those from the *Aspergillus* genus [12,19].

The antifungal mechanism of action of AgNPs is ascribed to multiple causes. AgNPs primarily interact with the fungal cell membrane, resulting in enhanced permeability and subsequent cellular apoptosis. This is enabled by the production of ROS that impair cellular functioning and metabolic processes. For instance, Moreno-Vargas et al. [58] demonstrated that AgNPs could agglomerate around fungal cell membranes, generating ROS that deactivates essential enzymes involved in nutrient exchange, ultimately causing cell dehydration and nutrient loss. Such mechanisms are likely responsible for the inhibition observed in the current study.

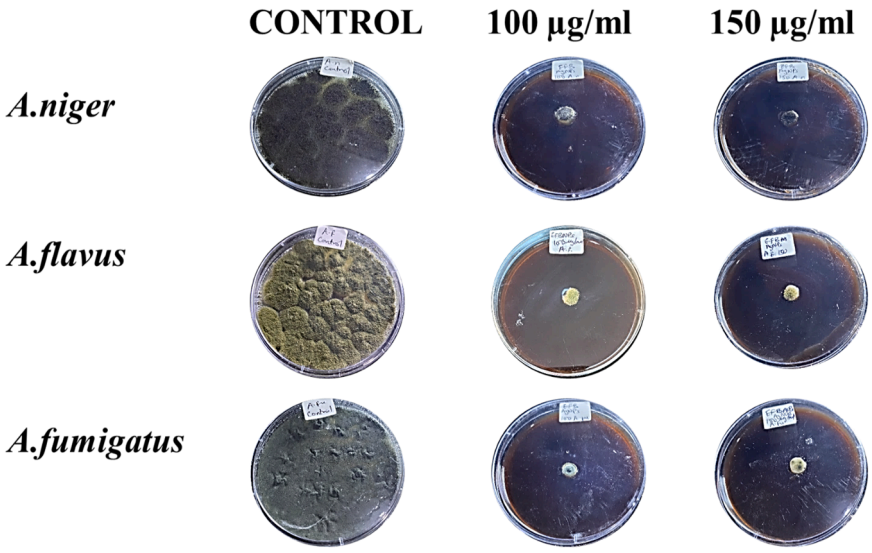


Fig. 5. Antifungal activity of biosynthesized EFB-AgNPs.

Similar to this study, Aguda and Lateef [6] reported that PBWW-AgNPs exhibited antifungal qualities, with inhibition rates varying between 67.50 % and 76.25 % at 100 and 150 µg/ml, highlighting that EFB-AgNPs achieve higher efficacy at the same concentration. This supports the notion that varieties of fungi can be efficiently inhibited by AgNPs produced utilizing environmentally friendly techniques, demonstrating the great potential of biosynthesized AgNPs as strong antifungal medications that might be utilized to treat illnesses brought on by resistant fungus.

3.4. Possible mechanism of action of the biosynthesized EFB-AgNPs on bacterial cells

The optical density (OD) values at 260 nm and 280 nm were higher in cultures that were treated with EFB-AgNPs than in normal cultures. This showed that nucleic acids and proteins were present (Table 1). This observation suggests that AgNPs compromise cellular integrity, leading to cell death, as has been reported by Abdellatif et al. [1] and Salmen and Alharbi [80]. The observed increase in optical density corresponds with the findings of Aguda and Lateef [6], further supporting that AgNPs disrupt cellular structures. One proposed mechanism is the ability of AgNPs to penetrate bacterial membranes and release Ag^{+} ions directly into the cytoplasm, enhancing antibacterial efficacy. Hossain et al. [39] demonstrated that AgNPs act as effective carriers for Ag^{+} ions, facilitating their passage across bacterial cell membranes. AgNPs can also compromise the structural integrity of bacterial cell walls and membranes, causing leakage of intracellular contents and leading to cell lysis [6,51].

Moreover, AgNPs are recognized for producing reactive oxygen species (ROS) when interacting with bacterial cells. These ROS can induce oxidative stress, resulting in damage to biological components like lipids, proteins, and DNA [10]. Oxidative damage significantly enhances the antibacterial activity of AgNPs by inducing cellular dysfunction and death. Additionally, the green synthesis of AgNPs using EFB extract may incorporate bioactive phytochemicals that synergistically boost the antibacterial efficacy of the nanoparticles [5]. These compounds stabilize the nanoparticles, preventing aggregation and maintaining antibacterial potency over time [57].

3.5. Anticoagulant activity of EFB-AgNPs

This study assessed the anticoagulant efficacy of EFB-AgNPs, which showed a considerable ability to obstruct blood coagulation. This discovery is consistent with the emerging evidence that AgNPs can alter the coagulation cascade, suggesting potential therapeutic benefits in settings requiring anticoagulation [15,4]. Three distinct samples were analyzed in the visual observations: blood combined with EFB-AgNPs, clotted blood (negative control), and blood mixed with EDTA (positive control) (Figure 6.1a). The tube containing blood with EFB-AgNPs had no evident clotting, indicating that these nanoparticles effectively inhibited coagulation. This suggests that EFB-AgNPs may interfere with the

coagulation process by interacting with clotting factors or chelating calcium ions, both of which are required for clotting. In contrast, the clotted blood in the negative control tube displayed the usual coagulation process. Simultaneously, the positive control, which included blood and EDTA, showed no clotting, which is consistent with EDTA's demonstrated anticoagulant properties. The microscopic investigation confirmed these findings (Figure 6.1b and c). The blood cells in the EDTA-treated sample were found to be dispersed and unaggregated, confirming the absence of clot formation. Similarly, the blood sample exposed to EFB-AgNPs showed no signs of clot formation, with blood

Table 1
Possible mechanism of action of the biosynthesized EFB-AgNPs on bacterial cells.

Organisms	Concentration (µg/ml)					
	100 µg/ml		150 µg/ml		CONTROL	
	260 nm	280 nm	260 nm	280 nm	260 nm	280 nm
Staphylococcus aureus	0.041	0.029	0.124	0.133	0.00	0.00
Klebsiella oxytoca	0.126	0.134	0.169	0.172	0.00	0.00
Escherichia coli	0.157	0.161	0.172	0.176	0.00	0.00
Pseudomonas aeruginosa	0.161	0.166	0.169	0.172	0.00	0.00
Proteus mirabilis	0.165	0.171	0.177	0.173	0.00	0.00

cells staying dispersed, showing the nanoparticles' anticoagulant characteristics. {{{Fig. 6}}}

EFB-AgNPs' anticoagulant impact may be due to their ability to bind and potentially delay essential coagulation cascade components such as thrombin or fibrinogen. Thrombin is a key enzyme in the clotting cascade, facilitating the conversion of fibrinogen to fibrin, which is necessary for clot formation [52]. EFB-AgNPs can successfully prevent clotting by inhibiting thrombin activity. Another possible mechanism is the chelation of calcium ions, which are required at numerous stages of the coagulation process [77]. EFB-AgNPs may potentially cause structural changes in blood proteins related with coagulation, reducing their efficacy. The findings suggest that EFB-AgNPs could be used as potential therapeutic agents for the prevention of thrombosis and other clot-related illnesses.

3.6. Thrombolytic activity of EFB-AgNPs

The visual data from the thrombolytic activity assay of EFB-AgNPs shows that the nanoparticles are effective at lysing blood clots (Figure 6.2). The initial image, "A," shows a tube with clotted blood, which serves as the negative control. The blood clot stays intact, with no signs of disintegration or lysis, indicating a normal coagulation process without the use of any thrombolytic agents. The second image, "B," shows a tube containing clotted blood and EFB-AgNPs. The blood clot in this sample has been completely dissolved, as evidenced by the liquid state of the blood, demonstrating that the nanoparticles successfully eliminate the fibrin network that causes clot formation. The high thrombolytic activity of EFB-AgNPs suggests that the nanoparticles have strong fibrinolytic properties. These findings are corroborated by the quantitative data shown in Table 2, which indicate that EFB-AgNPs have 100 % thrombolytic activity, since the whole thrombus was lysed, whereas the untreated control had 0 % activity.

The mechanism underlying this activity could involve the nanoparticles directly interacting with the clot's fibrin network, either by boosting the activation of endogenous fibrinolytic enzymes like plasmin or by directly degrading the fibrin structure [32]. The surface features of EFB-AgNPs, such as charge, size, and shape, may facilitate these interactions, hence increasing their ability to inhibit clot formation. Recent research indicates that the size and morphology of AgNPs may significantly alter their biological interactions, particularly their thrombolytic activity [81]. The ability of EFB-AgNPs to dissolve blood clots implies their potential use as a novel thrombolytic medicine, offering an alternative to standard thrombolytic treatments, which usually have significant side effects and limitations. The use of EFB-AgNPs may provide a more accurate and successful way for clot dissolution, particularly in the treatment of thrombotic diseases such as deep vein thrombosis, pulmonary embolism, and myocardial infarction.

3.7. In vitro antioxidant activities of EFB-AgNPs

3.7.1. DPPH (2,2-diphenyl-1-picrylhydrazyl) Assay

The DPPH assay was used to determine the antioxidant activity of EFB-AgNPs in comparison to ascorbic acid, a known antioxidant. The color shift in the DPPH solution containing EFB-AgNPs demonstrated the nanoparticles' radical scavenging ability. The color change from violet to bright yellow indicates the antioxidant capacity of the generated nanoparticles, which was then measured with a spectrophotometer. The results for EFB-AgNPs show a significant dose-dependent increase in activity showing significant differences between EFB-AgNPs and ascorbic acid across all tested concentrations ($p < 0.05$) (Fig. 7a). EFB-AgNPs showed 23.67 % scavenging activity at 100 μg/ml, increasing to 81.49 % at a maximum concentration of 160 μg/ml. Ascorbic acid, the positive control, demonstrated significantly higher activity at all concentrations, starting at 77.20 % at 100 μg/ml and reaching 93.27 % at 160 μg/ml. The gradual increase in activity revealed in this study is consistent with previous research that has demonstrated the antioxidant properties of AgNPs [13,21,25,63,90].

Comparable studies have showed increased DPPH scavenging

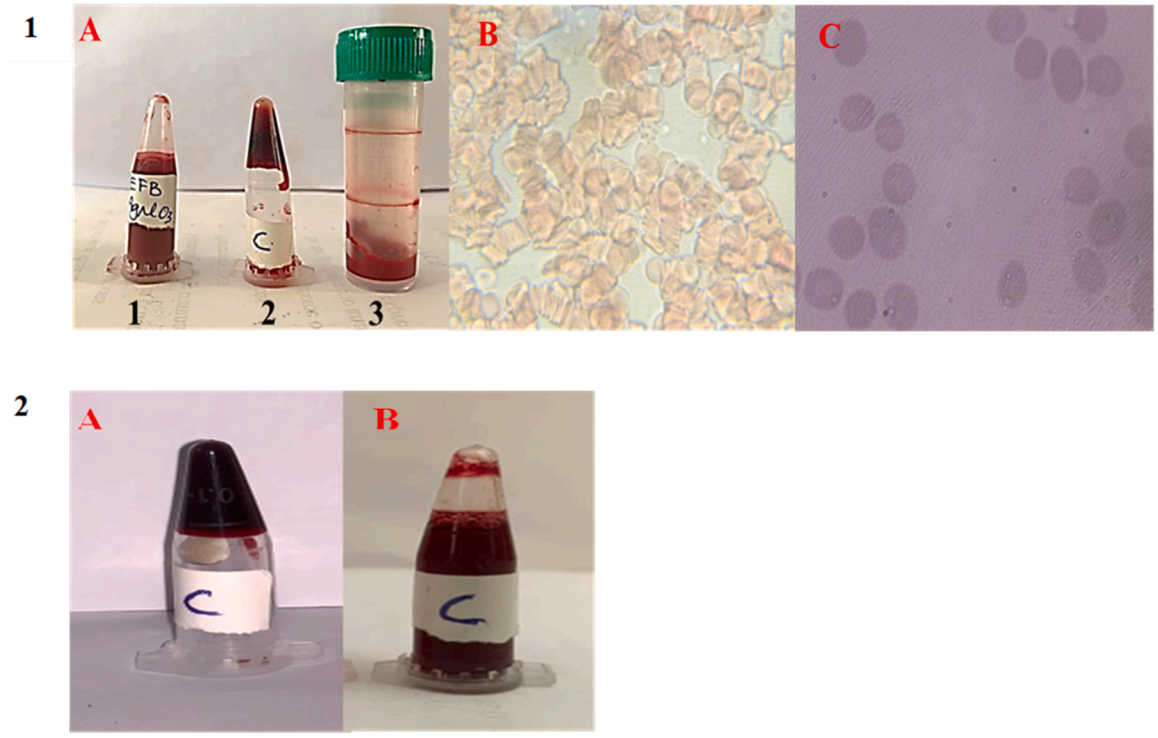


Fig. 6. Anticoagulant and thrombolytic activity of biosynthesized EFB-AgNPs. 1:(A: 1, blood + AgNPs; 2, negative control; 3, positive control); B: microscopic view of blood in positive control, at 40X; C: microscopic view of blood treated with EFB-AgNPs, at 40X. 2: (A: depicts the control sample, exhibiting clotted blood without treatment, in which the clot stays unaltered (0 % lysis); B: illustrates the EFB-AgNP-treated sample, exhibiting total clot breakdown (100 % thrombolytic activity)).

Table 2
Thrombolytic Activity of EFB-AgNPs.

Sample	Initial Tube Weight (a)	Tube + Clotted Blood (b)	Weight of Blood Clot (X = b - a)	Final Tube Weight (c)	Weight of Non-Lysed Blood (Y = c - a)	$Thrombolytic\ activity = \frac{X-Y}{X} x100$
Control (No treatment)	0.983 g	1.565 g	0.582 g	1.565 g	0.582 g	0 %
EFB-AgNPs Treated	0.983 g	1.565 g	0.582 g	0.983 g	0 g	100 %

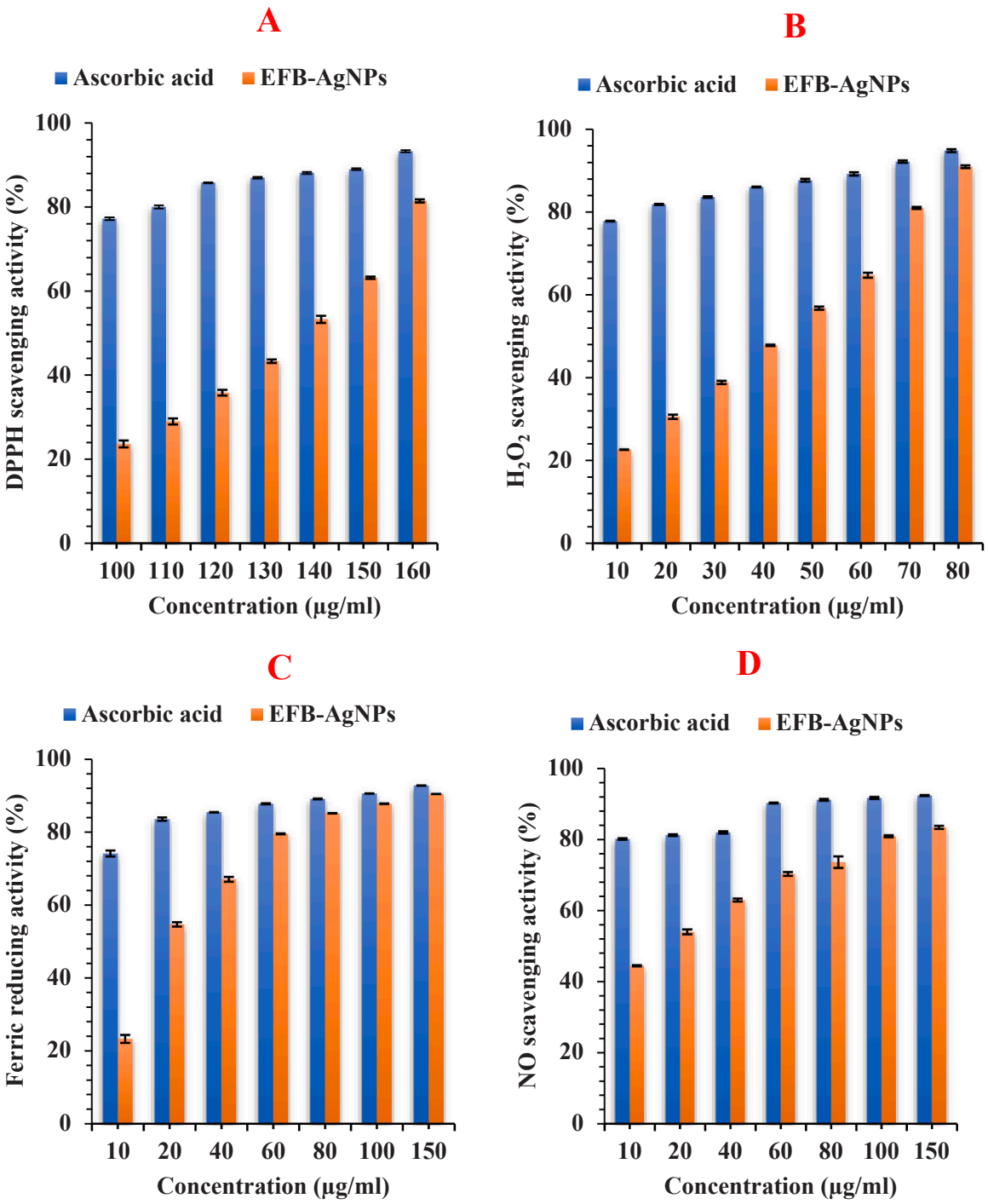


Fig. 7. Antioxidant activity of biosynthesized EFB-AgNPs: (A) DPPH activity, (B) H_2O_2 scavenging activity, (C) FRAP activity, and (D) NO scavenging activity. Data are expressed as mean ± SE from three independent experiments conducted in triplicate. Statistical analysis was performed using ANOVA with Duncan's test for mean comparison ($p < 0.05$). Error bars indicate the standard error of the mean.

efficacy at reduced doses. The scavenging activity of *Brachychiton populneus*-derived AgNPs, for instance, was 95 % at just 70 μg/ml, surpassing that of EFB-AgNPs at comparable and even higher doses [63]. In contrast, AgNPs made from *Rhodiola rosea* showed DPPH inhibition rates ranging from 50.66 % to 98.53 % over a wider concentration range of 10–450 μg/ml, according to [22]. While EFB-AgNPs showed strong scavenging action within a smaller range (100–160 μg/ml), highlighting their efficacy at low concentrations, RR-AgNPs obtained higher maximal inhibition but required larger concentrations. Similarly, [28] documented DPPH scavenging for *Fusarium nygamai* - derived AgNPs, achieving 66.91 % inhibition at 200 μg/ml. EFB-AgNPs displayed greater scavenging efficiency, reaching 81.49 % at 160 μg/ml compared to El-Ansary's results at higher concentrations. Differing phytochemical compositions and capping agents in the plant extracts utilized during synthesis may be the cause of this performance disparity, which can improve radical-scavenging capabilities.

3.7.2. Hydrogen peroxide (H_2O_2) scavenging activity

EFB-AgNPs were tested for their ability to scavenge H_2O_2 and compared to ascorbic acid. The results show a clear trend in H_2O_2 scavenging activity as the amounts of ascorbic acid and EFB-AgNPs increase (Fig. 7b). Ascorbic acid's scavenging activity ranges from 77.80 % at 10 μg/ml to 94.87 % at 80 μg/ml, while EFB-AgNPs show a corresponding increase from 22.62 % to 91.00 % at the same concentrations. This indicates that both ascorbic acid and EFB-AgNPs efficiently reduce oxidative stress by scavenging H_2O_2, a common ROS associated with a variety of clinical disorders. El-Ansary [28] reported that AgNPs derived from *Fusarium nygamai* exhibited H_2O_2 scavenging activity, with superior efficacy noted at higher concentrations. Notably, FN-AgNPs reached 70.3 % scavenging at 200 μg/ml, slightly below the performance of EFB-AgNPs at lower concentrations, indicating that EFB-AgNPs may achieve higher H_2O_2 neutralization efficiency within a moderate dosage range.

The mechanism by which AgNPs exhibit antioxidant effects is complex. According to research, the antioxidant properties of AgNPs are due to their large surface area and biomolecule stability, which may boost their interaction with free radicals like H_2O_2 [22,28]. Moreover, the antioxidant capabilities of AgNPs have been documented to exceed those of traditional antioxidants such as ascorbic acid in some scenarios, underscoring their potential as more effective free radical scavengers [28].The concentration-dependent improvement in scavenging activity reported for both ascorbic acid and EFB-AgNPs coincides with findings from previous studies that highlight the necessity of dosage in achieving optimal antioxidant effects [47,101].

3.7.3. Ferric reducing activity

The results from the ferric-reducing power assay for ascorbic acid and EFB-AgNPs demonstrate a clear relationship between antioxidant activity and the concentration of the tested substances (Fig. 7c). The study indicates that EFB-AgNPs have enhanced ferric-reducing capacity relative to ascorbic acid across all tested concentrations. At a concentration of 10 μg/ml, ascorbic acid demonstrates a ferric-reducing activity of 73.14 %, while EFB-AgNPs achieve merely 20.25 %. At a concentration of 150 μg/ml, ascorbic acid attains a maximum activity of 92.49 %, while EFB-AgNPs achieve 90.05 %. This suggests that while both compounds demonstrate antioxidant properties, ascorbic acid is a more effective ferric-reducing agent at lower concentrations.

The ferric-reducing power of a substance typically signifies its total antioxidant capability, since it demonstrates the capacity to donate electrons and convert ferric ions (Fe^{3+}) to ferrous ions (Fe^{2+}). This mechanism is crucial for alleviating oxidative stress by counteracting free radicals and ROS that can induce cellular damage. The observed concentration-dependent increase in reducing power aligns with prior studies indicating that antioxidant activity often follows this trend. ([28]) reported FN-AgNPs exhibited a 65.7 % reducing power at 200 μg/ml, substantially lower than EFB-AgNPs' 90.05 % at 160 μg/ml, suggesting EFB-AgNPs may achieve superior reducing power efficiency at moderate dosages. The ferric reduction capacity of EFB-AgNPs may be due to the unique properties of AgNPs, which possess inherent antioxidant qualities. The synthesis of AgNPs from EFB likely involves several phytochemicals that augment their antioxidant capabilities.

3.7.4. Nitric oxide assay

The nitric oxide (NO) scavenging efficacy of EFB-AgNPs was assessed and compared with the conventional antioxidant, ascorbic acid, at different concentrations (10–150 μg/ml) (Fig. 7d). Ascorbic acid, a powerful antioxidant, exhibited consistently higher scavenging activity, with a percentage oscillating from 80.18 % at 10 μg/ml to 92.38 % at 150 μg/ml. The EFB-AgNPs exhibited a dose-dependent improvement in NO scavenging activity, beginning at 44.50 % at the lowest concentration and attaining 83.43 % at 150 μg/ml. At concentrations of 10 and 20 μg/ml, the scavenging activity of EFB-AgNPs (44.50 % and 54.02 %, respectively) was markedly inferior to that of ascorbic acid (80.18 % and 81.24 %, respectively). As the concentration increased, the scavenging activity of EFB-AgNPs significantly improved, reaching 70.31 % at 60 μg/ml and 80.89 % at 100 μg/ml. At higher doses (150 μg/ml), the scavenging efficacy of EFB-AgNPs (83.43 %) approached that of ascorbic acid (92.38 %).

The capacity of EFB-AgNPs to scavenge nitric oxide radicals can be ascribed to the presence of AgNPs, which are known to possess antioxidant characteristics by neutralizing free radicals and mitigating oxidative stress. The progressive enhancement in scavenging activity with increasing concentrations suggests that the EFB-AgNPs can effectively mitigate nitric oxide-mediated oxidative stress at higher doses, which could have implications for their potential therapeutic applications in conditions involving oxidative stress and inflammation.

The comprehensive antioxidant evaluation of EFB-AgNPs, as shown by the DPPH, H2O2, FRAP, and NO tests, validates their strong, dose-dependent capacity to scavenge free radicals. Interestingly, the nanoparticles' capacity to lessen oxidative stress is consistent with results from prior investigations of plant-based AgNP, where phytochemical capping agents play a major role in increased antioxidant activity. The promise of EFB-AgNPs as a multipurpose antioxidant source is highlighted by this body of evidence, especially considering that they perform similarly to other common antioxidants like ascorbic acid.

3.8. Antidiabetic (alpha-amylase inhibitory) assay

The antidiabetic test of AgNPs derived from EFB demonstrates a dose-dependent enhancement in activity, indicating its efficacy in modulating blood glucose levels. At lower concentrations (20 μg/ml and 40 μg/ml), the antidiabetic efficacy of EFB-AgNPs is markedly minimal, exhibiting 10.5 % and 12.7 % inhibition, respectively, which is much inferior than ascorbic acid's effectiveness at 65.9 % and 69.1 %. Nevertheless, an increase in the concentration of EFB-AgNPs significantly enhances antidiabetic action. At a dose of 60 μg/ml, the nanoparticles exhibit a significant increase to 42.9 %, which escalates markedly at higher concentrations, attaining 66.8 % at 80 μg/ml and 84.9 % at 100 μg/ml. At this maximum concentration, the antidiabetic efficacy of EFB-AgNPs is equivalent to that of ascorbic acid (83.1 %), demonstrating its significant potency (Fig. 8). The concentration-dependent enhancement of inhibition found for EFB-AgNPs aligns with findings from earlier research that underscore the significance of dosage in attaining optimal antidiabetic effects. For instance, Qamar et al. [73] shown that higher concentrations of specific herbal extracts led to enhanced inhibition of alpha-amylase, underscoring the principle that successful antidiabetic therapies frequently depend on suitable dose. Likewise, a study by Ahmad [7] showed that the inhibitory efficacy of several natural substances on alpha-amylase increases at higher concentrations, hence corroborating the present findings.

This study aligns with the study of [25], who reported α-amylase inhibition of 82.43 % at 200 μg/ml and 85.75 % at 400 μg/ml for

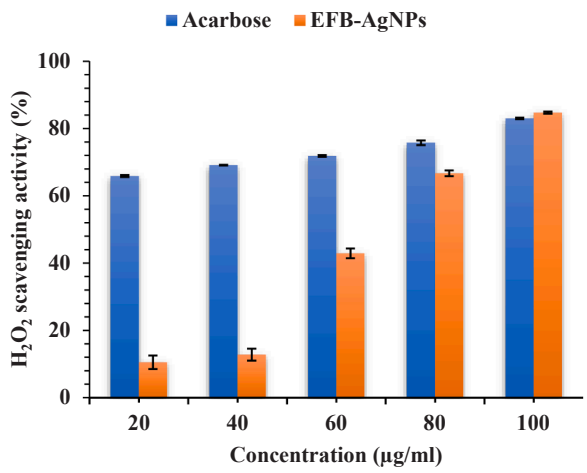


Fig. 8. Antidiabetic activity of biosynthesized EFB-AgNPs. Data are expressed as mean ± SE from three independent experiments conducted in triplicate. Statistical analysis was performed using ANOVA with Duncan's test for mean comparison ($p < 0.05$). Error bars indicate the standard error of the mean.

MA-AgNPs, indicating that EFB-AgNPs achieve similar efficacy at roughly half the concentration needed for MA-AgNPs. This efficiency may be attributed to the presence of bioactive compounds in EFB that enhance its alpha-amylase inhibitory properties. Prior research indicates that AgNPs derived from diverse plant extracts demonstrate considerable anti-diabetic properties, presumably attributable to the presence of bioactive chemicals such as flavonoids and phenolics that can engage with the enzyme [55]. Furthermore, the mechanism of alpha-amylase inhibition in this study likely involves competitive binding of the nanoparticles to the enzyme's active sites, reducing the breakdown of carbohydrates into glucose. Such enzyme inhibition can lower post-prandial blood glucose levels, which is beneficial for managing type 2 diabetes mellitus [2,75].

4. Conclusion

This study demonstrated the potential of agricultural waste in the sustainable manufacture of nanomaterials by effectively synthesizing silver nanoparticles (AgNPs) from empty fruit bunch (EFB) extract. The potent antibacterial, antioxidant, antidiabetic, anticoagulant, and thrombolytic properties of EFB-AgNPs were established by this innovative method. Thorough characterization demonstrated the nanoparticles' broad-spectrum biomedical applicability by confirming their stability, effectiveness, and structural integrity across assays. While EFB-AgNPs' antioxidant and antidiabetic actions highlight their applicability in treating oxidative stress and metabolic diseases, their antibacterial and antifungal qualities make them promising against multidrug-resistant infections. Crucially, this green synthesis technique promotes waste valorization and lessens the environmental effects usually connected to the manufacture of nanoparticles, which is in line with the circular bioeconomy principles. Our findings support EFB-AgNPs as versatile agents in nanotechnology, underscoring EFB's potential to foster high-value products aligned with the Sustainable Development Goals (SDGs) for Good Health and Well-being (SDG 3) and Responsible Production and Consumption (SDG 12). Integrating EFB within a circular bioeconomy framework effectively converts this waste from an environmental liability into a valuable resource, promoting sustainable innovation across various fields.

Funding

This research did not obtain specific financing from public, commercial, or non-profit entities.

CRediT authorship contribution statement

Bashirat Olamide Yusuf-Salihu: Writing – original draft, review and editing, Investigation, Validation, Supervision, methodology, Data curation, Conceptualization. **Shakirat Afodun Abdulmumini:** Writing – review and editing. **Taheeb Taiye Bajepade:** Resources and Investigation, Formal analysis. **Halimah Adekunbi Durosinmi:** Resources and Investigation, Formal analysis. **Muinat Olanike Kazeem:** Writing – review and editing. **Victoria Atinuke Ajayi:** Writing – review and editing. **Agbaje Lateef:** Validation, Writing – review and editing.

Declaration of Competing Interest

The authors declare that they have no known competing financial interests or personal relationships that could have appeared to influence the work reported in this paper.

Data availability

Data will be accessible upon request.

References

[1] A.A.H. Abdellatif, S.S. Alhathloul, A.S.M. Aljohani, H. Maswadeh, E.M. Abdallah, K.H. Musa, M.A.E. Hamd, Green synthesis of silver nanoparticles incorporated aromatherapies utilized for their antioxidant and antimicrobial activities against some clinical bacterial isolates, Bioinorg. Chem. Appl. 2022 (2022), https://doi.org/10.1155/2022/2432758.

[2] O.K. Abolaji, A.N. Ukwuani-Kwaja, I. Sani, M.N. Sylvester, In-vitro antidiabetic effect of *Ziziphus mucronata* leave extracts, J. Drug Deliv. Ther. 11 (2021) 9–13, https://doi.org/10.22270/jddt.v11i6-s.5216.

[3] M.A. Abu-Dalo, I.R. Al-Mheidat, A.W. Al-Shurafat, C. Grinham, V. Oyanedel-Craver, Synthesis of Silver Nanoparticles Using a Modified Tollens' Method in Conjunction With Phytochemicals and Assessment of Their Antimicrobial Activity, Peerj 7 (2019) e6413, https://doi.org/10.7717/peerj.6413.

[4] O.E. Adeyemi, O.A. Omoteso, T.O. Ajala, The in vitro biological activity of biosynthesized silver nanoparticles produced using *Mangifera indica* stem bark extract and properties of its pharmaceutical gel formulation, Bionanoscience 13 (2023) 638–649, https://doi.org/10.1007/s12668-023-01109-x.

[5] M.A. Adil, T. Khan, M. Aasim, A.A. Khan, M. Ashraf, Evaluation of the antibacterial potential of silver nanoparticles synthesized through the interaction of antibiotic and aqueous callus extract of *Fagonia indica*, Amb. Express 9 (2019), https://doi.org/10.1186/s13568-019-0797-2.

[6] O.N. Aguda, A. Lateef, Novel biosynthesis of silver nanoparticles through valorization of *Parkia biglobosa* fermented-seed wastewater: antimicrobial properties and nanotextile application, Environ. Technol. Innov. 24 (2021) 102077, https://doi.org/10.1016/j.eti.2021.102077.

[7] E. Ahmad, Isolation, structure elucidation and antidiabetic potential of *Rosa brunonii* L. fruit and fight diabetes with natural remedies, J. Chil. Chem. Soc. 68 (2023) 5887–5894, https://doi.org/10.4067/s0717-97072023000205887.

[8] F. Ahmadi, Green synthesis of silver nanoparticles from *Cannabis sativa*: properties, synthesis, mechanistic aspects, and applications, Chemengineering 8 (2024) 64, https://doi.org/10.3390/chemengineering8040064.

[9] H.E. Ahmed, Y. Iqbal, M.H. Aziz, M. Atif, Z. Batool, A. Hanif, N. Yaqub, W. A. Farooq, S. Ahmad, A. Fatehmulla, H. Ahmad, Green Synthesis of CeO2 Nanoparticles From the Abelmoschus Esculentus Extract: Evaluation of Antioxidant, Anticancer, Antibacterial, and Wound-Healing Activities, Molecules 26 (2021) 4659, https://doi.org/10.3390/molecules26154659.

[10] A. Aksoy, R. Alazragi, A.Y. Alabdali, R. Aljazzar, S.E. Sadi, M. Alostaz, M.E. Hindi, Antibacterial activity of metallic-core gold and silver nanoparticles against some animal pathogens, Ann. Anim. Sci. 23 (2023) 473–479, https://doi.org/10.2478/aoas-2023-0008.

[11] R. Algotiml, A. Gab-Alla, R. Seoudi, H.H. Abulreesh, M.Z. El-Readi, Elbanna, Anticancer and antimicrobial activity of biosynthesized red sea marine algal silver nanoparticles, Sci. Rep. 12 (2022), https://doi.org/10.1038/s41598-022-06412-3.

[12] N.M. Alhazmi, Fungicidal activity of silver and silica nanoparticles against Aspergillus Sydowii isolated from the soil in Western Saudi Arabia, Microorganisms 11 (2022) 86, https://doi.org/10.3390/microorganisms11010086.

[13] W.A.I. Al-Megrin, N.A. AlSadhan, D.M. Metwally, R. Al-Talhi, M.F. El-Khadragy, L.J.M. Abdel-Hafez, Potential antiviral agents of *Rosmarinus officinalis* extract against herpes viruses 1 and 2, Biosci. Rep. 40 (2020), https://doi.org/10.1042/bsr20200992.

[14] S.Y. Alomar, F. Albalawi, N. Arshi, S. Dwivedi, S. Kumar, N.M. Shaalan, N. Ahmad, Microwave mediated fast synthesis of silver nanoparticles and investigation of their antibacterial activities for gram-positive and gram-negative microorganisms, Crystals 11 (2021) 666, https://doi.org/10.3390/cryst11060666.

[15] U.U. Asuquo, *In-vitro* studies on the antidiabetic and antibacterial activity of biosynthesized silver nanoparticles with aqueous extract of *Moringa oleifera* leaf, J. Pharm. Bioresour. 21 (2024) 5–12, https://doi.org/10.4314/jpb.v21i1.2.
[16] M.A. Azeez, A. Lateef, T.B. Asafa, T.A. Yekeen, A. Akinboro, I.C. Oladipo, E. B. Gueguim-Kana, L.S. Beukes, Biomedical applications of cocoa bean extract-mediated silver nanoparticles as antimicrobial, larvicidal and anticoagulant agents, J. Clust. Sci. 28 (2017) 149–164, https://doi.org/10.1007/s10876-016-1055-2.
[17] J.A. Badmus, S.A. Oyemomi, O.T. Adedosu, T.A. Yekeen, M.A. Azeez, E. A. Adebayo, A. Lateef, U.M. Badeggi, S. Botha, A.A. Hussein, J.L. Marnewick, Photo-assisted bio-fabrication of silver nanoparticles using *Annona muricata* leaf extract: exploring the antioxidant, anti-diabetic, antimicrobial, and cytotoxic activities, Heliyon 6 (2020) e05413, https://doi.org/10.1016/j.heliyon.2020.e05413.
[18] J. Bagyalakshmi, Characterization and evaluation of green synthesized silver nanoparticles using *Moringa oleifera* leaf extract and its antihypertensive activity, Ann. Clin. Med. Case Rep. 13 (2024) 01–09, https://doi.org/10.47829/acmcr.2024.131602.
[19] B. Bakhshi, M. Sudhakar, L.S. Gowda, Garlic mediated green synthesis of silver nanoparticles as antifungal agents against Magnaporthe Oryzae, Indian J. Pharm. Educ. Res. 56 (2022) 1245–1252, https://doi.org/10.5530/ijper.56.4.207.
[20] A. Banu, M. Gousuddin, E.B. Yahya, Green synthesized monodispersed silver nanoparticles' characterization and their efficacy against cancer cells, Biomed. Res. Ther. 8 (2021) 4476–4482, https://doi.org/10.15419/bmrat.v8i8.686.
[21] S.M. Bhavi, B. Thokchom, M.B. Abbigeri, S.S. Bhat, S.R. Singh, P. Joshi, R. B. Yarajarla, Green synthesis, characterization, antidiabetic, antioxidant and antibacterial applications of silver nanoparticles from *Syzygium caryophyllatum* (L.) Alston leaves, Process Biochem 145 (2024) 89–103.
[22] B.-E. Bold, E. Urnukhsaikhan, T. Mishig-Ochir, Biosynthesis of silver nanoparticles with antibacterial, antioxidant, anti-inflammatory properties and their burn wound healing efficacy, Front. Chem. 10 (2022), https://doi.org/10.3389/fchem.2022.972534.
[23] A. Boondaeng, N. Khanoonkon, P. Vaithanomsat, W. Apiwatanapiwat, C. Trakunjae, P. Janchai, N. Niyomvong, Recovery and purification of fumaric acid from fermented oil palm empty fruit bunches using a simple two-stage precipitation procedure, Fermentation 8 (2022) 121, https://doi.org/10.3390/fermentation8030121.
[24] A. Bratovcic, Green synthesis of silver nanoparticles using aqueous orange and lemon peel extract and evaluation of their antimicrobial properties, Adv. Nanopart. 13 (2024) 11–28, https://doi.org/10.4236/anp.2024.132002.
[25] G. Chinnasamy, S. Chandrasekharan, S. Bhatnagar, Biosynthesis of silver nanoparticles from *Melia azedarach*: enhancement of antibacterial, wound healing, antidiabetic and antioxidant activities, Int. J. Nanomed. 14 (2019) 9823–9836, https://doi.org/10.2147/IJN.S231340.
[26] E. Dilipan, P. Sivaperumal, K. Kannan, R. Marimuthu, P. Vivekanandhan, Green synthesis of silver nanoparticles using seagrass *Cymodocea serrulata* (R.Br.) Asch. andAmp; magnus, characterization, and evaluation of anticancer, antioxidant, and antiglycemic index, Biotechnol. Appl. Biochem. 70 (2023) 1346–1356, https://doi.org/10.1002/bab.2444.
[27] F. Dimawarnita, Oil palm empty fruit leverage concerning delignification and fermentation in sheep, Adv. Anim. Vet. Sci. 12 (2024), https://doi.org/10.17582/journal.aavs/2024/12.1.180.188.
[28] A.E. El-Ansary, Green synthesized silver nanoparticles mediated by Fusarium nygamai isolate AJTYC1: characterizations, antioxidant, antimicrobial, anticancer, and photocatalytic activities and cytogenetic effects, Environ. Sci. Pollut. Res. 30 (2023) 100477–100499, https://doi.org/10.1007/s11356-023-29414-8.
[29] S. Faisal, A.A. Hamed, R.M. Shawky, M. Emara, Chitosan-silver nanoparticles: a versatile conjugate for biotechnological advancements, J. Adv. Pharm. Res. 7 (2023) 163–169, https://doi.org/10.21608/aprh.2023.218891.1222.
[30] N.S. Flores-Lopez, J.A. Cervantes-Chávez, D.G. Téllez de Jesús, M. Cortez-Valadez, M. Estévez-González, R. Esparza, Bactericidal and fungicidal capacity of Ag_2O/Ag nanoparticles synthesized with *Aloe vera* extract, J. Environ. Sci. Health Part A 56 (2021) 762–768, https://doi.org/10.1080/10934529.2021.1925492.
[31] K. Francis, Antibacterial activity of green synthesized silver nanoparticle using banana flower extract, Iop Conf. Ser. Mater. Sci. Eng. 1291 (2023) 012010, https://doi.org/10.1088/1757-899x/1291/1/012010.
[32] A. Gul, D. Ahmed, M.M. Fazil, T. Aslam, M. Rashid, H.M. Khan, A. Ali, S. Ali, Biofabrication of silver nanoparticles using *Spirulina platensis*: in vitro anti-coagulant, thrombolytic and catalytic dye degradation activity, Microsc. Res. Tech. 86 (2023) 823–833, https://doi.org/10.1002/jemt.24344.
[33] Q. Guo, T. Lan, G. Wu, Y. Chen, T. Xiao, Y. Xu, Z. Ma, M. Liao, X. Shen, Acidity-activated charge-convertible silver nanocomposites for enhanced bacteria-specific aggregation and antibacterial activity, Biomacromolecules 20 (2019) 3031–3040, https://doi.org/10.1021/acs.biomac.9b00598.
[34] A.F.A. HAMZAH, Evaluating the effect of low and high temperature mode of subcritical water pre-treated empty fruit bunches on co-digestion performance and kinetic study for methane production, Jopr (2023), https://doi.org/10.21894/jopr.2024.0030.
[35] W. Handayani, A. Listyarini, Y. Yasman, C. Imawan, A simple synthesis of silver nanoparticles on cellulose paper for antimicrobial applications, Mater. Sci. Forum 990 (2020) 191–196, https://doi.org/10.4028/www.scientific.net/msf.990.191.
[36] R.K. Harahap, Aspen plus simulation analysis of hydrogen production from biomass pyrolysis integrated with steam methane reformer unit, Iop Conf. Ser. Earth Environ. Sci. 1356 (2024) 012066, https://doi.org/10.1088/1755-1315/1356/1/012066.
[37] N.I.N. Haris, S. Sobri, Y.A. Yusof, N.K. Kassim, Innovative method for longer effective corrosion inhibition time: controlled release oil palm empty fruit bunch hemicellulose inhibitor tablet, Materials 14 (2021) 5657, https://doi.org/10.3390/ma14195657.
[38] Y. He, S. Chen, D. Xu, D. Ren, W. Xiyu, Fabrication of antimicrobial colorimetric pad for meat packaging based on polyvinyl alcohol aerogel with the incorporation of anthocyanins and silver nanoparticles, Packag. Technol. Sci. 36 (2023) 745–755, https://doi.org/10.1002/pts.2754.
[39] A. Hossain, X. Hong, E. Ibrahim, B. Li, G. Sun, Y. Meng, Y. Wang, Q. An, Green synthesis of silver nanoparticles with culture supernatant of a bacterium Pseudomonas Rhodesiae and their antibacterial activity against soft rot pathogen *Dickeya dadantii*, Molecules 24 (2019) 2303, https://doi.org/10.3390/molecules24122303.
[40] A. Irawan, Potential and opportunity of co-firing power plant in indonesia through torrefaction of empty fruit bunch (EFB) - a review, WCEJ Untirta 5 (2021) 25, https://doi.org/10.48181/wcej.v5i1.12139.
[41] Z.N. Jafar, Biosynthesis of silver nanoparticles using ethanolic extract of the marine alga *Enteromorpha intestinalis* and evaluation of their antibacterial activity, Egypt. J. Aquat. Biol. Fish. 28 (2024) 735–756, https://doi.org/10.21608/ejabf.2024.350083.
[42] I. Jasso-Ruiz, U. Velazquez-Enriquez, R.J. Scougall-Vilchis, R.A. Morales-Luckie, T. Sawada, R. Yamaguchi, Silver nanoparticles in orthodontics, a new alternative in bacterial inhibition: in-vitro study, Prog. Orthod. 21 (2020), https://doi.org/10.1186/s40510-020-00324-6.
[43] R. Javed, S. Ijaz, H. Hameed, M. Nazish, M.S. Sharif, A. Afreen, K.M. Alarjani, M. S. Elshikh, S. Mehboob, S.A. Razak, A. Waheed, R. Ahmed, M. Tariq, Phytochemical-mediated biosynthesis of silver nanoparticles from strobilanthes glutinosus: exploring biological applications, Micromachines 14 (2023) 1372, https://doi.org/10.3390/mi14071372.
[44] M.O. Kazeem, A.P. Titilope, A.B. Agbaje, G.E. Ogunleye, Laccase facilitated synthesis of silver nanoparticles for biomedical, biocontrol and dye degradation applications, Bima J. Sci. Technol. 8 (2024) 2536–6041, https://doi.org/10.56892/bima.v8i1.593.
[45] P. Khandel, S.K. Shahi, D. Soni, R.K. Yadaw, L. Kanwar, Alpinia calcarata: potential source for the fabrication of bioactive silver nanoparticles, Nano Converg. 5 (2018), https://doi.org/10.1186/s40580-018-0167-9.
[46] S.R. Kumar, Antimicrobial properties of green synthesized silver and chitosan nanocomposites, Bioinformation 19 (2023) 745–748, https://doi.org/10.6026/97320630019745.
[47] A.H. Labulo, O.A. David, A.D. Terna, Green synthesis and characterization of silver nanoparticles using *Morinda lucida* leaf extract and evaluation of its antioxidant and antimicrobial activity, Chem. Pap. 76 (2022) 7313–7325, https://doi.org/10.1007/s11696-022-02392-w.
[48] A. Lateef, B.I. Folarin, S.M. Oladejo, P.O. Akinola, L.S. Beukes, E.B. Gueguim-Kana, Characterization, antimicrobial, antioxidant, and anticoagulant activities of silver nanoparticles synthesized from *Petiveria alliacea* L. leaf extract, Prep. Biochem. Biotechnol. 48 (2018) 646–652, https://doi.org/10.1080/10826068.2018.1479864.
[49] A. Lateef, K.O. Ismaheel, O.O. Ajani, D.A. Adebayo, S.T. Fagbemiro, T.B. Asafa, E. B. Gueguim-Kana, L.S. Beukes, S.H. Abbas, H.M. Irshad, Kolanut-mediated magnesium oxide nanostructures for biomedical applications: antimicrobial, antioxidant, larvicidal, anticoagulant and thrombolytic activities, South Afr. J. Bot. 159 (2023) 334–343, https://doi.org/10.1016/j.sajb.2023.06.026.
[50] K.D. Lee, P. Kuppusamy, D.H. Kim, G. Nagarajan, G.P. Maniam, K.C. Choi, Forage crop lolium multiflorum assisted synthesis of AgNPs and their bioactivities against poultry pathogenic bacteria in *in-vitro*, Indian J. Microbiol. 58 (2018) 507–514, https://doi.org/10.1007/s12088-018-0755-8.
[51] Y. Li, Polyethyleneimine surface-modified silver-selenium nanocomposites for anti-infective treatment of wounds by disrupting biofilms, Biomed. Mater. 19 (2024) 045016, https://doi.org/10.1088/1748-605x/ad4e84.
[52] T. Li, W. Huang, H. Yu, Synergetic antimicrobial effect of silver nanoparticles conjugated with iprodione against Valsa Mali, Materials 15 (2022) 5147, https://doi.org/10.3390/ma15155147.
[53] N. Liaqat, N. Jahan, Khalil-ur-Rahman, T. Anwar, H. Qureshi, Green synthesized silver nanoparticles: optimization, characterization, antimicrobial activity, and cytotoxicity study by hemolysis assay, Front. Chem. 10 (2022), https://doi.org/10.3389/fchem.2022.952006.
[54] S. Macieja, B. Środa, B. Zielińska, S. Roy, A. Bartkowiak, Łopusiewicz, Bioactive carboxymethyl cellulose (CMC)-based films modified with melanin and silver nanoparticles (AgNPs)—the effect of the degree of CMC substitution on the in-situ synthesis of agnps and films' functional properties, Int. J. Mol. Sci. 23 (2022) 15560, https://doi.org/10.3390/ijms232415560.
[55] S. Majeed, M. Danish, N.A. Zakariya, R. Hashim, M.T. Ansari, S. Alkahtani, M. S. Hasnain, In vitro evaluation of antibacterial, antioxidant, and antidiabetic activities and glucose uptake through 2-NBDG by Hep-2 liver cancer cells treated with green synthesized silver nanoparticles, Oxid. Med. Cell. Longev. 2022 (2022) 1–14, https://doi.org/10.1155/2022/1646687.
[56] A.A. Mathews, K.K. Bijoy, Can silver nanoparticles be an answer to combat the drug resistance? Ip, Int. J. Med. Microbiol. Trop. Dis. 4 (2020) 149–151, https://doi.org/10.18231/2581-4761.2018.0033.
[57] M.G. Moghadam, A. Bagherzade, F. Ghorbanzade, M.Y. Hanafi-Bojd, M. Yousefi, In-vitro antibacterial activity of glass ionomer cements containing silver nanoparticles synthesized from leaf extract of Mentha piperita, Dent 10 (2022) 3000, https://doi.org/10.5195/d3000.2022.267.
[58] J.M. Moreno-Vargas, L.M. Echeverry-Cardona, L.E. Moreno-Montoya, E. Restrepo-Parra, Evaluation of antifungal activity of Ag nanoparticles

synthetized by green chemistry against *Fusarium solani* and *Rhizopus stolonifera*, Nanomaterials 13 (2023) 548, https://doi.org/10.3390/nano13030548.
[59] I. Mukhlisa, M. Masfria, S. Sumaiyah, Synthesis of silver nanoparticles (Agnp) from the extract of Kemloko Fruit (*Phyllantus emblica* L.), Int. J. Sci. Technol. Manag. 3 (2022) 1329–1333, https://doi.org/10.46729/ijstm.v3i5.620.
[60] M. Muryanto, F. Amelia, M.N. Izzah, R. Maryana, E. Triwahyuni, T.B. Bardant, E. Filailla, Y. Sudiyani, M. Gozan, Delignification of empty fruit bunch using deep eutectic solvent for biobased-chemical production, Iop Conf. Ser. Earth Environ. Sci. 1108 (2022) 012013, https://doi.org/10.1088/1755-1315/1108/1/012013.
[61] F. Mustapha, E. Ella, S. Luka, Y. Wada, Phytochemical constituents and GC-MS profiling of the whole plant ethanol extract of *Thesium viride* Hill and its oral toxicity in Balb/C mouse model, UMYU J. Microbiol. Res. UJMR 8 (2023) 31–38.
[62] Nam, N.H., 2021. Multifunctional Silver Nanoparticles: Synthesis and Applications. ⟨https://doi.org/10.5772/intechopen.96712⟩.
[63] M. Naveed, H. Batool, S. ur Rehman, A. Javed, S.I. Makhdoom, T. Aziz, A. A. Mohamed, M.Y. Sameeh, M.W. Alruways, A.S. Dablool, A.A. Almalki, A. S. Alamri, M. Alhomrani, Characterization and evaluation of the antioxidant, antidiabetic, anti-inflammatory, and cytotoxic activities of silver nanoparticles synthesized using *Brachychiton populneus* leaf extract, Processes 10 (2022) 1521, https://doi.org/10.3390/pr10081521.
[64] M.C.D. Niluxsshun, K. Masilamani, U. Mathiventhan, Green Synthesis of Silver Nanoparticles From the Extracts of Fruit Peel of Citrus Tangerina, Citrus Sinensis, and Citrus Limon for Antibacterial Activities, Bioinorg. Chem. Appl. 2021 (2021) 1–8, https://doi.org/10.1155/2021/6695734.
[65] Noah, A.S., 2022. Oil Palm Empty Fruit Bunches (OPEFB) – Alternative Fibre Source for Papermaking. ⟨https://doi.org/10.5772/intechopen.98256⟩.
[66] O.H. Obiazikwor, H.O. Shittu, Antibacterial activity of silver nanoparticles synthesized using *Citrus sinensis* peel extract against pathogens isolated from diseased tomato (Solanum lycopersicum L.), Bact. Emp. 4 (2021) 1–3, https://doi.org/10.36547/be.2021.4.1.1-3.
[67] I.C. Oladipo, A. Lateef, M.A. Azeez, T.B. Asafa, T.A. Yekeen, S.B. Ogunsona, H. M. Irshad, S.H. Abbas, Antidiabetic properties of phytosynthesized gold nanoparticles (AuNPs) from *Datura stramonium* seed, IOP Conf. Ser. Mater. Sci. Eng. 805 (2020) 012035, https://doi.org/10.1088/1757-899X/805/1/012035.
[68] M. Oves, M.A. Rauf, M. Aslam, H.A. Qari, H. Sonbol, I. Ahmad, G.S. Zaman, M. Saeed, Green synthesis of silver nanoparticles by *Conocarpus lancifolius* plant extract and their antimicrobial and anticancer activities, Saudi J. Biol. Sci. 29 (2022) 460–471, https://doi.org/10.1016/j.sjbs.2021.09.007.
[69] N. Pal, S. Agrawal, Green synthesis of silver nanoparticles using *Ocimum tenuiflorum* leaf extract and its antimicrobial activity against certain pathogens, Int. J. Life Sci. Pharma Res. (2022), https://doi.org/10.22376/ijpbs/lpr.2021.11.1.l148-154.
[70] P. Parvekar, J. Palaskar, S. Metgud, R. Maria, S.D. Dutta, The minimum inhibitory concentration (MIC) and minimum bactericidal concentration (MBC) of silver nanoparticles against *Staphylococcus aureus.* Biomater. Investig. Dent. 7 (2020) 105–109, https://doi.org/10.1080/26415275.2020.1796674.
[71] R.C. Pețu, A.-F. Săracu, C.-V. Ungureanu, Green synthesis of metal nanoparticles using microalgae: a review, Ann. "Dunarea Jos" Univ. Galati Fascicle Ix Metall. Mater. Sci. 45 (2022) 16–19, https://doi.org/10.35219/mms.2022.3.03.
[72] R. Pradeep, N.P. Muralidharan, Comparative study of anti microbial activity of dose dependent silver nanoparticle preparation, iodophor and chlorhexidine against extended spectrum beta lactamase strains, J. Pharm. Res. Int. (2020) 32–36, https://doi.org/10.9734/jpri/2020/v32i2630837.
[73] S. Qamar, K. Hussain, N.I. Bukhar, S.Z. Siddique, Aziz-Ur-Rehman, M. Abbas, S. Parveen, A. Latif, A. Qamar, E. Ali, N. Shehzadi, M.R. Islam, S. Naheed, Evaluating the antidiabetic and antioxidant properties of 5- benzyl-1,3,4-oxadiazole-2-thiol, Trop. J. Pharm. Res. 18 (2021) 1095–1100. ⟨https://doi.org/10.4314/tjpr.v18i5.26⟩.
[74] S. Qamer, M.H. Romli, F. Che-Hamzah, N. Misni, N. Joseph, N.A.A. Al-Haj, S. A. Nordin, Systematic review on biosynthesis of silver nanoparticles and antibacterial activities: application and theoretical perspectives, Molecules 26 (2021) 5057, https://doi.org/10.3390/molecules26165057.
[75] A. Quazi, M. Patwekar, F. Patwekar, S. Alghamdi, B.S. Rajab, A.O. Babalghith, F. Islam, In vitro alpha-amylase enzyme assay of hydroalcoholic polyherbal extract: proof of concept for the development of polyherbal teabag formulation for the treatment of diabetes, Evid. Based Complement. Altern. Med. 2022 (2022) 1–7, https://doi.org/10.1155/2022/1577957.
[76] R. Álvarez-Chimal, Green Synthesis of Nanoparticles: A Biological Approach (2023). https://doi.org/10.5772/intechopen.1002203.
[77] K. Rajesh, Biosynthesis of silver nanoparticles from marine actinobacterium *Micromonospora* Sp. and their bioactive potential, Cureus (2024), https://doi.org/10.7759/cureus.53870.
[78] N.S.A. Rasid, A. Shamjuddin, N.A.S. Amin, Chemical and structural changes of ozonated empty fruit bunch (EFB) in a ribbon-mixer reactor, Bull. Chem. React. Eng. Catal. 16 (2021) 383–395, https://doi.org/10.9767/bcrec.16.2.10506.383-395.
[79] V. Sagar, R.R. Patel, S. Singh, M. Singh, Green synthesis of silver nanoparticles: methods, biological applications, delivery and toxicity, Mater. Adv. 4 (2023) 1831–1849, https://doi.org/10.1039/d2ma01105k.
[80] S.H. Salmen, S.A. Alharbi, Silver nanoparticles synthesized biogenically from *Aloe Fleurentiniorum* extract: characterization and antibacterial activity, Green. Chem. Lett. Rev. 13 (2020) 1–5, https://doi.org/10.1080/17518253.2019.1707883.
[81] P. Salve, A. Vinchurkar, R. Raut, R. Chondekar, J. Lakkakula, A. Roy, M. J. Hossain, S. Alghamdi, M. Almehmadi, O. Abdulaziz, M. Allahyani, A. S. Dablool, M.M.R. Sarker, M.F.N. Azlina, An evaluation of antimicrobial, anticancer, anti-inflammatory and antioxidant activities of silver nanoparticles synthesized from leaf extract of *Madhuca longifolia* utilizing quantitative and qualitative methods, Molecules 27 (2022) 6404, https://doi.org/10.3390/molecules27196404.
[82] A.M.E. Shafey, Green synthesis of metal and metal oxide nanoparticles from plant leaf extracts and their applications: a review, Green. Process. Synth. 9 (2020) 304–339, https://doi.org/10.1515/gps-2020-0031.
[83] W.A. Shaikh, S. Chakraborty, G. Owens, R.U. Islam, A review of the phytochemical mediated synthesis of AgNP (silver nanoparticle): the wonder particle of the past decade, Appl. Nanosci. 11 (2021) 2625–2660, https://doi.org/10.1007/s13204-021-02135-5.
[84] Shehla, A review, tabulation of the antimicrobial effect of silver nanoparticles, Iop Conf. Ser. Mater. Sci. Eng. 1248 (2022) 012110, https://doi.org/10.1088/1757-899x/1248/1/012110.
[85] T. Siddiqui, M.K. Zia, M. Muaz, H. Ahsan, F.H. Khan, Synthesis and characterization of silver nanoparticles (AgNPs) using chemico-physical methods, IJCA Indones. J. Chem. Anal. 6 (2023) 124–132, https://doi.org/10.20885/ijca.vol6.iss2.art4.
[86] N.M. Silviana, The potential effect of silver nanoparticles to inhibit microbial activity in orthodontic adhesive appliances: a literature review, Insisiva Dent. J. Maj. Kedokt. Gigi Insisiva 13 (2024) 56–63, https://doi.org/10.18196/di.v13i1.21886.
[87] B. Sitorus, M.B. Malino, Electrical conductivity of conducting polymer composites based on conducting polymer/natural cellulose, Elkha 13 (2021) 84, https://doi.org/10.26418/elkha.v13i1.46048.
[88] T.R. Srinophakun, P. Suwajittanont, Techno-economic analysis of bioethanol production from palm oil empty fruit bunch, Int. J. Technol. 13 (2022) 1787, https://doi.org/10.14716/ijtech.v13i8.6131.
[89] S. Suhartati, I.S. Saputra, D. Rahmi, Y. Yulizar, S. Sudirman, Bioreduction and characterization of silver nanoparticles from oil palm empty fruit bunch, J. Sains Mater. Indones. 21 (2020) 177, https://doi.org/10.17146/jsmi.2020.21.4.6032.
[90] H. Tahir, F. Rashid, S. Ali, M. Summer, M. Afzal, Synthesis, characterization, phytochemistry, and therapeutic potential of *Azadirachta indica* conjugated silver nanoparticles: a comprehensive study on antidiabetic and antioxidant properties, Biol. Trace Elem. Res. (2024), https://doi.org/10.1007/s12011-024-04293-3.
[91] F. Tariq, N. Ahmed, M. Afzal, M.A.U. Khan, B. Zeshan, Synthesis, characterization and antimicrobial activity of bacillus subtilis-derived silver nanoparticles against multidrug-resistant bacteria, Jundishapur J. Microbiol. 13 (2020), https://doi.org/10.5812/jjm.91934.
[92] Tuzyuk, N.V., Pokryshko, O., 2022. Microbiological Substantiation of the Use of Xenografts Saturated with Silver Nanocrystals for the Treatment of Burn Wounds. Шпитальна Хірургія Журнал ІМені Л Я Ковальчука 12–18. ⟨https://doi.org/10.11603/2414-4533.2022.1.12912⟩.
[93] R.M. Varghese, Antimicrobial activity of silver nanoparticles synthesized using *Ocimum tenuiflorum* and *Ocimum gratissimum* herbal formulations, Cureus (2024), https://doi.org/10.7759/cureus.54994.
[94] B. Venkatadri, E. Shanparvish, M.R. Rameshkumar, M.V. Arasu, N.A. Al-Dhabi, V. K. Ponnusamy, P. Agastian, Green synthesis of silver nanoparticles using aqueous rhizome extract of *Zingiber officinale* and *Curcuma longa*: *in-vitro* anti-cancer potential on human colon carcinoma HT-29 cells, Saudi J. Biol. Sci. 27 (2020) 2980–2986, https://doi.org/10.1016/j.sjbs.2020.09.021.
[95] W.B. Wang, C.-Y. Pan, E.-Y. Huang, B.-J. Peng, J.C. Hsu, J. Clapper, Electrospun polyacrylonitrile silver nanoparticle (PAN-AgNP) nanocomposites as alternative, Antimicrob. Mater. (2022), https://doi.org/10.26434/chemrxiv-2022-jbg4p-v2.
[96] K. Wu, H. Li, X. Cui, R. Feng, W. Chen, Y. Jiang, C. Tang, Yaohai Wang, Yan Wang, X. Shen, Y. Liu, M. Lynch, Mutagenesis and resistance development of bacteria challenged by silver nanoparticles, Antimicrob. Agents Chemother. 66 (2022), https://doi.org/10.1128/aac.00628-22.
[97] Q. Yang, Green synthesis of silver nanoparticles using *Jasminum nudiflorum* flower extract and their antifungal and antioxidant activity, Nanomaterials 13 (2023) 2558, https://doi.org/10.3390/nano13182558.
[98] K.E. Yunusov, A.A. Sarymsakov, J. Jalilov, Physicochemical properties and antimicrobial activity of nanocomposite films based on carboxymethylcellulose and silver nanoparticles, Polym. Adv. Technol. 32 (2021) 1822–1830, https://doi.org/10.1002/pat.5223.
[99] N.A. Yusuf-Omoloye, F.M. Adeyemi, W.F. Sule, L. Azeez, O.O. Oyedara, A. A. Wahab, O.H. Ajigbewu, A. Lateef, Green-synthesis, characterization, and antibacterial activity of *Azanza garckeana* seed extract silver nanoparticles against vancomycin-resistant Enterococci, Nanotechnol 6 (2024) 100035, https://doi.org/10.1016/j.nxnano.2023.100035.
[100] B.O. Yusuf-Salihu, S.A. Abdulmumini, A.T. Ajao, Fermented rice water for biosynthesis of silver nanoparticles (AgNPs) and its antimicrobial activities against microorganisms associated with skin infection, Niger. J. Microbiol. 37 (2023) 6578–6587.
[101] B.O. Yusuf-Salihu, A. Lateef, L. Azeez, Phytochemical profiling of wastes from the processing of shea butter (*Vitellaria paradoxa*) and pharmacological potentials within the paradigm of circular bioeconomy: Emphasizing antioxidant and antidiabetic applications, Clean. Circ. Bioeconomy 9 (2024) 100107, https://doi.org/10.1016/j.clcb.2024.100107.
[102] M.K. Zaman, A.M. Azzeme, S.N. Ramli, N.A. Shaharuddin, S. Ahmad, S.N. A. Abdullah, Solvent extraction and its effect on phytochemical yield and antioxidant capacity of woody medicinal plant, *Polyalthia bullata*, BioResources 15 (2020) 9555.
[103] S.Y.S. Zeebaree, O.I.H. Zebari, A.Y.S. Zeebaree, D.A. Hussein, E.H. Hanna, Rapid detection of mercury ions using sustainable natural gum-based silver nanoparticles, Catalysts 12 (2022) 1464, https://doi.org/10.3390/catal12111464.